



Review

Clinical applications of 7 T MRI in the brain

Anja G. van der Kolk^{a,*}, Jeroen Hendrikse^{a,1}, Jaco J.M. Zwanenburg^{a,b,2}, Fredy Visser^{a,c,2}, Peter R. Luijten^{a,2}^a Department of Radiology, University Medical Center Utrecht, Postbox 85500, 3508 GA Utrecht, The Netherlands^b Image Sciences Institute, University Medical Center Utrecht, The Netherlands^c Philips Healthcare, Best, The Netherlands

ARTICLE INFO

Article history:

Received 6 July 2011

Accepted 12 July 2011

Keywords:

MRI

High field

Neuroradiology

Brain anatomy

7 T

ABSTRACT

This review illustrates current applications and possible future directions of 7 Tesla (7 T) Magnetic Resonance Imaging (MRI) in the field of brain MRI, in clinical studies as well as clinical practice. With its higher signal-to-noise (SNR) and contrast-to-noise ratio (CNR) compared to lower field strengths, high resolution, contrast-rich images can be obtained of diverse pathologies, like multiple sclerosis (MS), brain tumours, aging-related changes and cerebrovascular diseases. In some of these diseases, additional pathophysiological information can be gained compared to lower field strengths. Because of clear depiction of small anatomical details, and higher lesion conspicuousness, earlier diagnosis and start of treatment of brain diseases may become possible. Furthermore, additional insight into the pathogenesis of brain diseases obtained with 7 T MRI could be the basis for new treatment developments. However, imaging at high field comes with several limitations, like inhomogeneous transmit fields, a higher specific absorption rate (SAR) and, currently, extensive contraindications for patient scanning. Future studies will be aimed at assessing the advantages and disadvantages of 7 T MRI over lower field strengths in light of clinical applications, specifically the additional diagnostic and prognostic value of 7 T MRI.

© 2011 Elsevier Ireland Ltd. Open access under the [Elsevier OA license](http://www.elsevier.com/locate/elsevier).

1. Introduction

Magnetic Resonance Imaging (MRI) is a versatile technique to image changes in brain anatomy and function. Since its clinical emergence in the beginning of the eighties, magnetic field strength for clinical MRI has increased from <0.5 T to a wide use of 3.0 T in current clinical practice today. Foremost, increase in signal to noise and susceptibility induced contrast at higher field strengths is especially useful for imaging techniques that require a high signal-to-noise (SNR) and contrast-to-noise (CNR) ratio, such as functional imaging techniques (fMRI) and MR spectroscopy, but can also be used for high resolution anatomical imaging, including 3-dimensional (3D) volume imaging, within acceptable scanning time. Although not widely used clinically at this point in time, an increasing number of research sites worldwide have access to MRI

scanners with a field strength of 7.0 T. Most of the current research on these 7 T MRI platforms is related to hardware- and sequence optimization to address some of the technical challenges of (ultra) high field imaging (inhomogeneous transmit field, increased susceptibility artefacts, specific absorption rate (SAR) limitations). To date only a few clinical studies have been performed at this ultra-high field strength, and there is an active debate in the MR community [1,2] if and when 7 T MRI may become the field strength of choice for certain clinical applications.

The emphasis of most (technical) developments at 7 T lies on imaging the brain. Functional imaging (BOLD) and techniques that exploit susceptibility induced contrast are among the ones that benefit most from the ultra-high field strength, and the artefacts in the brain are less pronounced than in other areas of the body. However, a widespread acceptance of ultra-high field imaging as a clinical diagnostic instrument will require high quality anatomical imaging sequences, like T_1/T_2 -weighted, T_2^* -weighted, Fluid-Attenuated Inversion Recovery (FLAIR)-imaging and Magnetic Resonance Angiography (MRA). Combined with increased SNR and CNR generated at these higher field strengths, 7 T MRI may find its way to many improved and even new clinical applications.

Recently, a number of 3D anatomical sequences have been developed and optimized that make optimal use of the increased SNR at 7 T [3–6]. These sequences include FLAIR imaging, which is an important sequence in most diagnostic standard brain MRI

* Corresponding author at: Department of Radiology, University Medical Center Utrecht, Heidelberglaan 100, Postbox 85500, 3508 GA Utrecht, The Netherlands. Tel.: +31 887550286; fax: +31 302581098.

E-mail addresses: A.G.vanderKolk@umcutrecht.nl (A.G. van der Kolk), J.Hendrikse@umcutrecht.nl (J. Hendrikse), J.J.M.Zwanenburg@umcutrecht.nl (J.J.M. Zwanenburg), F.Visser-2@umcutrecht.nl (F. Visser), P.Luijten@umcutrecht.nl (P.R. Luijten).

¹ Tel.: +31 887556687; fax: +31 302581098.

² Tel.: +31 887551234; fax: +31 302581098.

protocols due to its high CNR between brain tissue lesions of any sort and the surrounding healthy brain tissue. Although not as important as the FLAIR sequence, T_2^* -weighted MRI sequences are increasingly used in clinical MRI protocols as well, for instance for the detection of microbleeds. At 7 T, the larger susceptibility effect compared to MRI at lower field strengths may result in new clinical applications of this sequence. Furthermore, T_1 -weighted imaging, especially after contrast administration, can provide more detail to assess small pathology not seen as clearly at lower field strength, for instance lesions of the intracranial vessel wall. Finally, MR angiography, which is regularly used in clinical practice to assess all kinds of brain pathology, can be obtained with an ultra-high resolution for optimal assessment of even smaller arteries of the brain than at lower field strengths, like the perforating lenticulostriate arteries.

Besides increased costs and limited availability, disadvantages for clinical use of 7 T MRI include a range of imaging artefacts that to date has prevented a further widespread dissemination of ultra-high field MRI for clinical diagnosis. Moreover, we still have to learn how normal anatomy and diseases look like with the changes in contrast and resolution at high field. These could very well be the main reasons that the published literature on clinical research at 7 T has thus far been limited. The aim of this current review article is to show the clinical potential of 7 T MR high-resolution anatomical brain imaging based on the current state of the art imaging platforms and the use of (high field) dedicated pulse sequences. Advanced hardware modification (e.g. the use of multi-transmit technology), which undoubtedly will further improve the clinical performance of ultra-high field imaging, is beyond the scope of this review. Apart from a review of the current literature, a series of illustrative patient examples will be included.

2. Technical aspects of high field 7 T imaging

For a given contrast, the three fundamental factors that determine the design and applications of MR imaging are: signal-to-noise ratio (SNR), imaging speed, and spatial resolution (Fig. 1). These factors are all related, and changing one of them will affect the other two parameters and vice versa. This provides flexibility to utilize the increased intrinsic SNR at high field, which rises approximately linearly with field strength. Within boundary conditions (like limits on tissue heating), the increased SNR can be used for either better lesion conspicuousness, or for increasing imaging speed to reduce motion artefacts (which facilitates imaging of unstable or less cooperative patients), or for increasing the spatial resolution to identify smaller pathological lesions. Even though many pathological processes in the brain in daily clinical routine can be detected with lower-resolution images, one can think of many applications where higher resolution could be beneficial. High-resolution imaging could make it possible to detect brain diseases in an early stage, by visualizing very small pathological changes. Furthermore, the pathological basis and development of brain diseases could be further elucidated by more detailed imaging.

High magnetic field strength also affects the relaxation times of tissues, T_1 and T_2^* in particular [7]. Fortunately, as shown by Rooney et al. [8], the increased longitudinal relaxation times still allow for sufficient contrast between grey and white matter in T_1 -weighted brain imaging. Even more so, as the T_1 -values for grey and white matter increase from 1.5 T to 7 T from 1188 ms and 656 ms to 2132 ms and 1220 ms, respectively [8], high field imaging can be used to generate exquisite Time-Of-Flight MR Angiography (TOF-MRA) with a high contrast-to-noise. In TOF-MRA, tissues with static spins become excited several times by radiofrequency (RF) pulses within their relaxation time T_1 , and become saturated. Non-excited flowing blood that enters the excited volume, on the other hand,

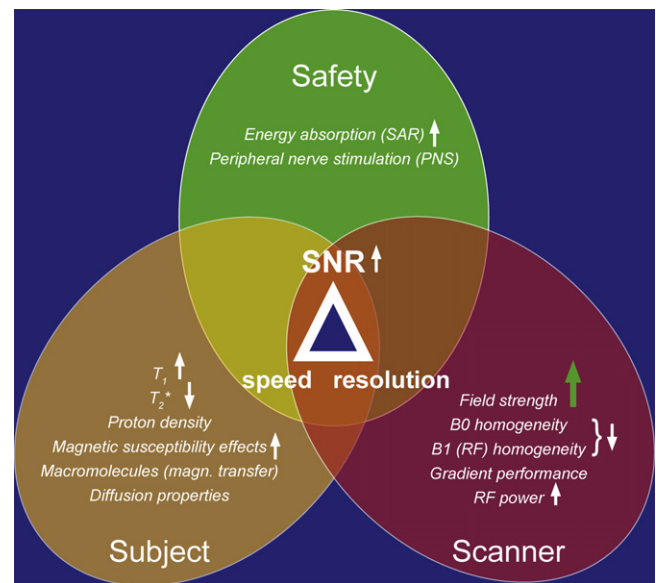


Fig. 1. Within MRI, for a certain contrast there is a central trade-off between signal-to-noise ratio (SNR), resolution and imaging speed (faster imaging comes at the cost of losing resolution and/or SNR, for example), which takes place within boundary conditions imposed by the scanner, the subject and safety considerations. This graph illustrates the changes (white arrows) that occur when the strength of the static field of the MRI scanner is increased (green arrow up). When the field strength of the MRI scanner is increased, the intrinsic SNR increases, which can be exchanged for either increased imaging speed (e.g. by acquiring less averages) or increased resolution. Since the tissue relaxation parameters and the susceptibility effects depend on the field strength, also the contrasts will change at higher field. Challenges are imposed by the increased inhomogeneity of both the main field (B_0) and the RF transmit field (B_1), together with an increase in SAR.

will be excited for only a limited number of times, depending on the chosen slab volume, resulting in a high signal. For a given pulse angle, when the T_1 relaxation times of tissues become longer, the static spins will relax less in between the RF pulses, resulting in lower signal of static tissue, and hence in a better contrast between suppressed background and flowing blood.

The shortened T_2^* -values are related to the increased magnetic susceptibility effects that scale linearly with magnetic field strength, while T_2 -value changes will be not as pronounced. Also, the magnetic susceptibility effects of tissues at higher field cause more distortion of the local magnetic field in its surrounding. Especially, paramagnetic and diamagnetic substances like deoxyhaemoglobin (veins), calcium (calcified tumour), blood degradation products (like haemosiderin in microbleeds), iron-depositions and air (air-filled cavities) will exert this effect. Although these enhanced susceptibility effects may cause image distortions and/or local signal drop-outs (due to dephasing), it also gives the opportunity of creating better tissue contrast. This can be readily visualized with a T_2^* -weighted sequence sensitive for susceptibility effects.

Besides these intrinsic MR characteristics of tissue that change as a function of field strength, there are certain conditions that impose a boundary condition for the design and application for diagnostic high-field imaging protocols. Because of the larger magnetic susceptibility effects seen at high field strength, metallic objects like surgical implants, and air such as in the nasal cavities, will cause much more image distortion and artefacts (signal drop-out) than at lower field strengths for a given receive bandwidth. Possible temperature effects in conducting implant materials are another impediment for the widespread clinical use of high-field imaging. Obviously, these effects impose strict safety measures for MRI at all field strengths and, albeit much more pronounced at high field, should be taken into consideration in all MRI applications. At this point in time, it is still not clear what effect metallic

implants have when placed in a high magnetic field: most studies on safety of metallic objects have been performed at 1.5 or 3 T. Safety precautions regarding 7 T MRI so far state that nothing metallic should enter the bore, since it would be expected that the shorter wavelength at 7 T ‘matches’ more easily with metallic objects, causing resonance and heating. Currently, this is the major contraindication when conducting patient studies at 7 T. Although patients can be screened for the presence of for instance dental prostheses, it is very labourious, and often practically impossible to track if operation clips or other metallic implants like stents have been used for patients with a history of surgery, and if these type of clips or stents are safe. Also, in elderly patients, especially patients with atherosclerosis-related diseases such as stroke, the presence of stents in the heart, aorta or leg vasculature is common and not always specifically documented if implanted a long time ago. To illustrate the size of the current problem, in a recent stroke study we had to exclude 173 of 611 eligible stroke- or transient ischemic attack (TIA)-patients due to 7 T MRI contraindications [9]. Safety testing of most often used operation clips, stents and dental implants is important to decrease the present list of contraindications.

Finally, at high magnetic field, severe inhomogeneity in the applied transmit field (RF field) is seen. Because of this inhomogeneity, the achieved pulse angle will vary between locations in the brain. This results in a spatially varying SNR [10]. More importantly, and dependent on the sequence that is used, this might lead to deviation of the contrast obtained from different locations in the image. These effects are most pronounced at the temporal lobes of the brain and the cerebellum. Therefore, in the peripheral areas of the brain assessment of anatomical structures and possible pathology is currently difficult. Furthermore, the inhomogeneous transmit field causes additional SAR restrictions. The global SAR (mean SAR over a certain volume) increases approximately with the square of the applied magnetic field strength. However, because of the inhomogeneities of the transmit field, the SAR is also less homogeneously distributed over the brain [11], causing larger differences between areas and higher SAR peaks at specific places, further imposing stringent limitations on the duty cycle of the applied sequences. The challenges in the transmit field can be addressed with new hardware approaches as well as improved pulse sequence design. This review will describe MRI applications based on this latter approach only to present data that can be obtained by most clinical 7 T platforms today.

3. Clinical 7 T studies in the literature

The four most important disease areas in the literature studied with 7 T MRI are multiple sclerosis (MS), cerebrovascular diseases (microbleeds, aneurysms), brain tumours, and degenerative diseases like dementia and Parkinson’s disease. In MS studies, the detection of (sub)cortical lesions is important in unravelling the pathogenesis of MS lesions in general. In cerebrovascular diseases most attention is paid to MR angiography at high resolution to show small (lenticulostriate) arteries feeding the deep brain structures. Also, the role of microbleeds in this disease category has been studied quite extensively. In tumour patients most attention is paid to visualization of the microvasculature with T_2^* -weighted imaging. For degenerative diseases like dementia, clinical 7 T MRI studies mainly focus on technical developments for high-resolution imaging of the hippocampus. The current state of research and potential future directions within these clinical fields will be discussed below. Furthermore, the status of 7 T MRI in other areas like epilepsy and accidental findings will be discussed.

3.1. Multiple sclerosis

Since the introduction of MR imaging in human clinical practice, multiple sclerosis (MS) has always been a prominent application field for new MR sequences and other technical developments. Several reasons could explain this interest, like the availability of clinical follow-up, participation in other studies simplifying contact and inclusion, and the relative young age of MS patients (20–30 s) decreasing the prevalence of contraindications for MRI such as metallic implants. Another important reason might be the often difficult diagnosis of this disease, heightening the need for new diagnostic imaging modalities. MS is a demyelinating disease with a currently almost unknown pathogenesis, and few evidence-based measurable biomarkers which can be used to predict both disease course and treatment effect. Most applications of MRI in the assessment of MS have focused on imaging white matter lesions, one of the possible hallmarks of MS. Although white matter lesions can be found at lower field strength throughout the brain, cortical lesions remain a challenge because of the lower resolution that can be attained at lower field strength, and the reduced contrast between the lesion and its surrounding tissue. However, recent work has shown that these cortical lesions could be of particular importance to gain more insight into the pathogenesis of MS [12].

Moving to high-field MRI could provide the spatial resolution and CNR needed to visualize these cortical lesions with higher precision. However, the main sequences that are used for imaging MS lesions at lower field strengths are FLAIR or double inversion-recovery (DIR). These sequences are not easily implemented at higher field, like 7 T MRI, and require rigorous sequence changes. Recently, our group have shown the availability of a new 3D FLAIR-sequence at 7 T [3,13], offering the opportunity to study lesions with high anatomical detail, possibly giving more insight into the pathological processes of MS. Recent work by de Graaf et al. [14] has shown the better conspicuity of MS lesions at 7 T FLAIR compared to 3 T FLAIR MRI (Fig. 2). Several studies showed the possibility of imaging cortical MS lesions with other high-resolution sequences, like T_2^* -weighted, double inversion recovery (DIR) and MPRAGE imaging [15–18]. Some lesions were shown to possess additional characteristics like peripheral susceptibility rings not seen before on lower field strengths [15,16]. Possibly detection of cortical lesions and other hallmark features may increase the correlation between clinical disease progression and MRI imaging features, although no such study has been performed yet.

Apart from these recent advances in FLAIR-imaging and in imaging cortical lesions, several studies have shown with T_2^* -weighted imaging a relationship between veins and the presence of MS-related white matter lesions [19–22]. In MS-related white matter lesions, veins were found in 80–85% of patients compared to 10–20% in normal-aging-related white matter lesions [21,22]. From a pathophysiological point of view this association between white matter lesions and (central) veins might be important, although from previous studies at lower field strength as well as post-mortem studies this relation has already been known [23]. Comparison between 7 T and 3 T MRI showed that the relation between veins and MS-related white matter lesions was more clear at 7 T with a higher percentage of lesions showing a vein with T_2^* -weighted imaging [21]. In this regard detection of a central vein within a lesion may help in definitively diagnosing MS when the diagnosis is uncertain, although no study yet has proven that 7 T MRI is better in diagnosing MS compared to 3 T MRI.

3.2. Cerebrovascular diseases

Clinical studies within the field of cerebrovascular diseases have mainly focused on high-resolution MRA and imaging of

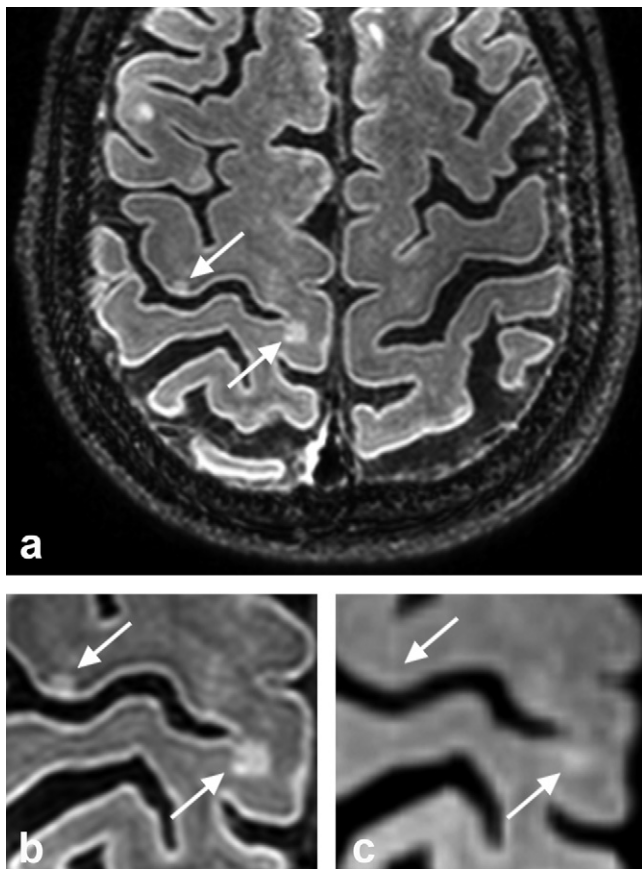


Fig. 2. 63-year-old female with primary progressive multiple sclerosis (MS) with an Expanded Disability Status Score (EDSS) of approximately 6.0. A 7 T MRI scan was performed for the detection of possible cortical lesions. a, Axial overview and b, zoomed-in image of a high parietal cortical MS lesion (right arrow) on axial 7 T 3D-FLAIR sequence. In retrospect, this lesion could also be seen on the 3 T 3D-FLAIR images, although with lower contrast-to-noise (c). The other cortical lesion (left arrow) on the other hand could not be seen at 3 T MRI. Imaging parameters 7 T 3D-FLAIR as previously published [3], 0.8 mm isotropic resolution; 3 T FLAIR 1.1 mm isotropic.

Courtesy of W.L. de Graaf, VUmc Amsterdam, The Netherlands.

microbleeds with T_2^* -weighted sequences. Following the development of high resolution MRA at 7 T, which could show lenticulostriate arterial branches [24–26], these methods have been applied in patient studies. The lenticulostriate arteries are the small arterial branches which feed the deep brain structures such as the basal ganglia. The presence of lacunar infarcts in these areas is thought to be related to the pathological state of these small arteries, also referred to as small vessel disease [27]. Thus far, small vessel disease could almost solely be inferred indirectly from the presence of white matter lesions and lacunar infarcts which are thought to be imaging markers for the presence and severity of disease of the small arterial vasculature [27]. Because of its high SNR and, thereby, its possibility to image at a high spatial resolution, 7 T made it possible to visualize more direct markers for small vessel disease, i.e. the pathological arteries themselves. This has therefore been an increasing field of interest. In one study the number and configuration of lenticulostriate arteries was compared between controls and chronic stroke patients, who showed less arteries than the control group [28]. In patients with hypertension the number of visible lenticulostriate arteries was also found to be smaller compared to controls [29]. In patients with CADASIL these arteries were not found to differ from control subjects even in the presence of severe white

matter lesions or lacunar infarcts [30]. It should be realized that, although 7 T MRI can show the perforating arteries over a certain length, these arteries are still large-sized arteries compared to the even smaller resistance arterioles, which are still out of reach of inflow-based MRA methods. It is therefore possible that the small artery disease causing white matter lesions and smaller lacunar infarcts is currently still out of reach of the available 7 T MRI methods.

The appearance of aneurysms can also be assessed with high-resolution MRA, where studies [31,32] have shown the clear depiction of characteristics of the aneurysm including the presence of small perforating branches. These branches, when originating from the aneurysm, could potentially result in an infarct if not noticed when planning treatment, for instance clipping of the aneurysm. Only two studies have compared 1.5 T and 7 T TOF-MRA for the conspicuousness of aneurysms, where the image quality was rated better at 7 T [31,32]. However, in terms of sensitivity for the detection of small aneurysms, no comparisons have been made with 1.5 T and 3 T MRI, and it has therefore yet to be determined if 7 T MRI may detect more clinically relevant aneurysms. For follow-up of treated aneurysms 7 T MRI is currently not possible due to the contraindications of clips and coils.

In the last decade, microbleeds have attracted more and more attention, especially at higher field strengths like 3 T and 7 T MRI. Due to their paramagnetic nature – consisting of blood breakdown products – microbleeds can be successfully visualized using T_2^* -weighted imaging. The increased sensitivity of higher field MRI for microbleeds is caused both by the increased susceptibility effect at a higher magnetic field strength, and by the increased spatial resolution that can be attained. Because of the large susceptibility effect at 7 T, visualization of microbleeds is possible even with very short echo times (TE), retaining most of the background signal and causing a large CNR. For example, in some healthy volunteer-studies microbleeds were even visible at TE = 2.5 ms [33]. By increasing spatial resolution, even smaller microbleeds can also be visualized. With lower resolution, and often lower field strength, the slight hypointensity of small microbleeds may be lost in the noise. It has been found that detection of microbleeds was superior at 7 T compared to 1.5 T MRI [34].

Microbleeds may show the pathophysiology of small vessel disease from a different angle compared to white matter lesions and lacunar infarcts. Second, they could be a marker for increased risk of bleeding when an ischemic stroke is treated with intravenous thrombolysis. Furthermore, microbleeds may also be related to the presence of hypertension. In a 7 T MRI case example microbleeds were found to be located close to lenticulostriate arteries in a patient with a hypertensive haemorrhage [35]. However, the exact cause of (very small) microbleeds detected with 7 T MRI, and their role in cerebrovascular diseases needs to be further elucidated before clinical implementation, especially at 7 T, can be commenced. Although short echo times are advantageous for assessing microbleeds, with longer echo times the strong susceptibility effect of veins can be used to make venograms, and assess the venous tree and its relation to pathology like microbleeds in more detail.

Another area that has attracted more interest in the last few years is the presence of intracranial atherosclerosis. Visualization of the arterial lumen only gives information regarding possible stenosis, but does not give information regarding the nature of this stenosis; for this you need to visualize the intracranial vessel wall itself. At 1.5 T and 3 T MRI the intracranial vessel wall could only be depicted when large atherosclerotic lesions or a vasculitis was present [36–38]. The high SNR at 7 T may be exploited for an increased resolution that makes it possible to depict this intracranial vessel wall. A study with 7 T MRI showed visualization of the intracranial vessel wall, also in healthy condition. Future

studies could show whether intracranial atherosclerotic lesions have a higher prevalence in patients who suffered from a stroke or transient ischemic attack [9].

3.3. Degenerative brain diseases

7 T MRI in degenerative diseases has so far focused on two subjects: dementia (Alzheimer's disease (AD) and vascular dementia) and Parkinson's disease. One study assessed the association between vascular dementia and the presence of white matter lesions and microbleeds on T_2^* -weighted and FLAIR imaging, where 7 T could potentially improve detection, diagnosis and treatment of vascular dementia with T_2^* -weighted sequences [39]. Cerebral microbleeds may be present as part of the spectrum of cerebral amyloid angiopathy [40]. Although potentially important, the real prognostic value of microbleeds in patients with dementia and Alzheimer's disease has yet to be determined.

The holy grail of 7 T MRI in degenerative brain diseases is the direct detection of amyloid plaques. Very sensitive imaging methods such as T_2^* -weighted imaging employed at a very high resolution may show changes in the brain tissue that may be related to the presence of amyloid. In a post-mortem study 7 T MRI showed the presence of such very small tissue changes in the cerebral cortex [41]. Still, it is not clear if the (cortical) tissue changes detected in post-mortem studies can be reproduced in patient studies where shorter imaging times (i.e. lower spatial resolution) and patient motion are potential problems that should be overcome [42].

Other studies on dementia focus on evaluation of the detailed substructures of the hippocampus. In several comparative studies it has been shown that 7 T MRI can show more anatomical detail in the hippocampus compared to 1.5 T [43] and 3 T [44] MRI, by means of higher contrast between grey and white matter substructures. The detection of these substructures may be important because changes in the hippocampus associated with memory loss may be more pronounced in specific areas of the hippocampus. Currently it is not clear which 7 T MRI sequence(s) is (are) best in showing these substructures, although T_1 -, FLAIR, T_2^* - and T_2 -weighted imaging at high resolution showed promises in this regard [4,43,44]. Based on lower clinical field strengths it can be expected that coronal FLAIR-based imaging approaches may be of value. Still, for 7 T MRI the medial temporal lobe and the hippocampus are located in a difficult area of the brain in which field inhomogeneities are often present and SAR-constraints may limit image quality. Already with the currently available imaging methods, differences in hippocampal substructures between control subjects and patients with probable AD were demonstrated [44]. From a pathophysiological point of view imaging of these differences may be important in understanding which substructures of the hippocampus are involved in memory loss in dementia and AD, including the role they play in the pathogenesis and their possible role as marker for progression to AD in patients with minor memory complaints.

Finally, several studies with 7 T MRI have been performed in patients with Parkinson's disease (PD), directed at imaging deep brain stimulation targets, like the subthalamic nucleus and internal globus pallidus, and at visualization of the substantia nigra, thought to play a primary role in the pathogenesis of PD. Treatment of PD by means of deep brain stimulation depends greatly on correct positioning of the stimulating electrode in the target areas. Cho et al. [45] showed that 7 T MRI was superior in delineating these areas compared to 1.5 T and 3.0 T. Bajaj et al. [46] showed that 7 T MRI could distinguish subregions of the substantia nigra, and found an increased iron content in a part of this basal ganglion in PD patients compared to healthy volunteers. Recently, Oh et al. [47] visualized differences in anatomical patterns of the substantia nigra between

healthy controls and PD patients with 7 T MRI, possibly enabling earlier diagnosis of PD.

3.4. Brain tumours

In clinical brain tumour imaging the presence or absence of MRI-enhancement after administration of a gadolinium-based contrast agent is still the most important imaging marker to discriminate between low- and high-grade tumours. Although distinction between tumour grades with this marker is not perfect, as a general rule low-grade brain tumours show no contrast enhancement in comparison to high-grade tumours. This contrast enhancement is predominantly caused by blood-brain-barrier disruption with subsequent contrast leakage. Better tumour grading and characterization may be relevant for treatment planning and guiding biopsy. It is well known that brain tumours are heterogeneous and, depending on the location a biopsy is taken, a different tumour grade may be found. With respect to tumour enhancement comparisons between 7 T MRI and lower field strengths have shown no differences in presence and size of the enhancing region after contrast administration [48,49]. With other MRI methods like T_2^* -weighted imaging, 7 T may provide additional information relative to 3 T and 1.5 T MRI. For instance, 7 T MRI may show details of the arterial cerebral microvasculature in brain tumours [48,49], and provide additional information regarding delineation of more rare tumours [50]. Venography by means of T_2^* -weighted imaging may provide information about tumour metabolism, since the increased metabolism in a brain tumour may result in increased oxygen consumption resulting in more deoxyhaemoglobin and therefore more pronounced veins on T_2^* -weighted MRI sequences.

There are still unexplored areas within the field of brain tumour imaging that could be of potential interest to researchers working with 7 T MRI. Expansion of tumour in areas surrounding the tumour core is difficult to assess with standard MRI methods. It is well known, based on tumour recurrence after treatment, that areas surrounding the tumour core are also infiltrated by tumour tissue. In these areas oedema is usually present, which is visualized as high signal on T_2 -weighted imaging sequences such as T_2 -weighted FLAIR MRI. If new imaging methods at 7 T could help determine the extent of tumour infiltration in these surrounding areas of oedema, this could be very important for a more aggressive treatment of these areas (surgically or with radiotherapy) to avoid tumour recurrence after initial treatment. Also, differentiation between necrotic primary brain tumours, necrotic metastases and cerebral abscesses with current imaging techniques is still a diagnostic dilemma. All three show ring-like enhancement after contrast administration, and often have the same characteristics on for instance diffusion-weighted imaging. Using new sequences at 7 T with different contrasts compared to lower field strength, might show promise in further elucidating differences between these three pathologically very different entities. Furthermore, after initial treatment an important area of diagnostic uncertainty is the differentiation between radionecrosis and tumour recurrence. Both radionecrosis (a treatment effect) and tumour recurrence can show enhancement after contrast administration. Although several MRI methods have been developed at lower field strength for the differentiation between both entities [51], there may be room for improvements of these methods. Unfortunately, the post-operative status of patients with this diagnostic dilemma (metal craniofixatives, etc.) hampers performing potentially interesting patient studies on the differentiation between radionecrosis and tumour recurrence with newly developed 7 T MRI methods. Currently, only initial studies have been performed in smaller series of brain tumour patients at 7 T [48–50,52] and it is not clear yet if 7 T MRI can solve important issues such as tumour infiltration better than existing MRI methods at lower field strengths.

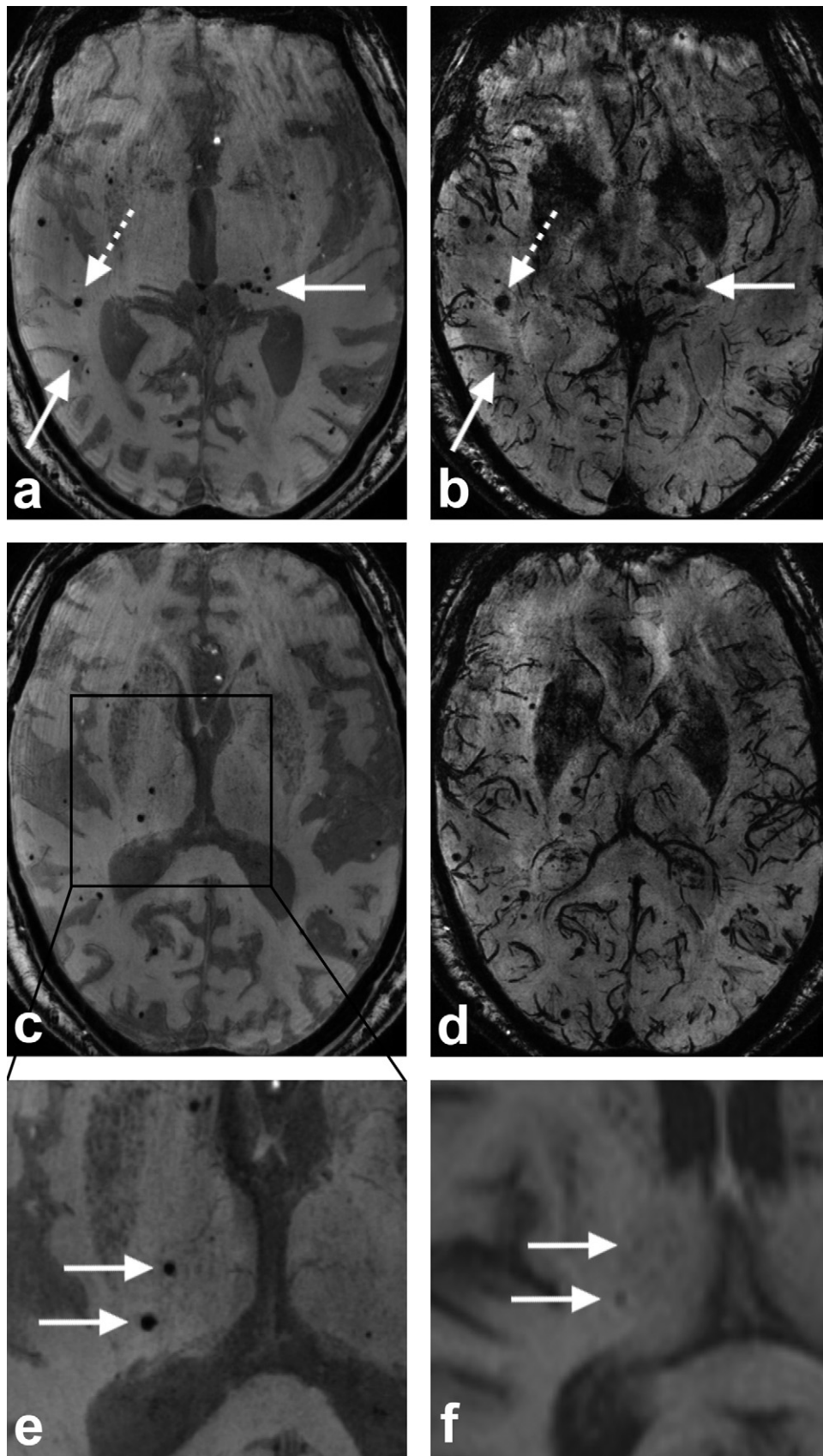


Fig. 3. 77-year-old man with a history of hypertension presented with transient dysphasia based on a transient ischemic attack (TIA) of the left hemisphere. a, c, Axial minimal intensity projections (minMIPs) over 10 mm thick volumes of the 1st and b, d, minMIPs of the 2nd echo of 7 T T_2^* -weighted images, where multiple microbleeds can be found throughout the brain (arrows). Some are less easily distinguished on the 2nd echo minMIPs due to overlapping venous structures (striped arrows) and artefacts close to the nasal cavity. e, Zoomed-in image of 7 T and f, of standard clinical 1.5 T 1st echo minMIPs, showing better visualization of the microbleeds due to the increased susceptibility effects at 7 T compared to 1.5 T MRI. Imaging parameters as previously published [33].

Courtesy of Dr. M.M. Conijn, VUmc Amsterdam, The Netherlands.

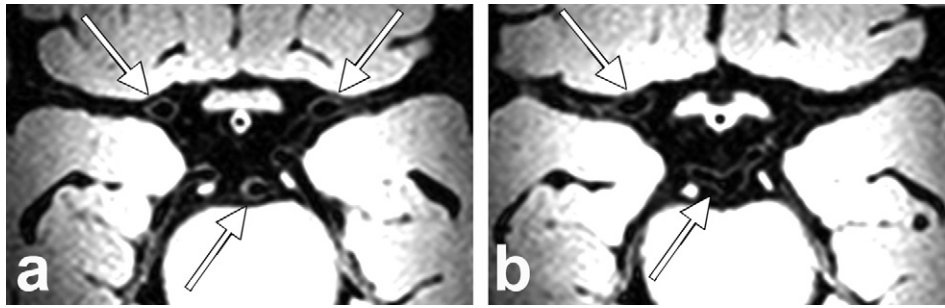


Fig. 4. 62-year-old female with a history of smoking and hyperlipidemia presented with transient monocular visual field defect of the left eye, based on amaurosis fugax. a, b, Axial MPR-TSE images, showing healthy intracranial arterial vessel wall of both internal carotid arteries and basilar artery (a, arrows), as well as the M1 of the right middle cerebral artery (b, arrow) and the basilar artery-posterior cerebral artery bifurcation (b, arrow). Imaging parameters as previously published [9], 0.8 mm isotropic resolution.

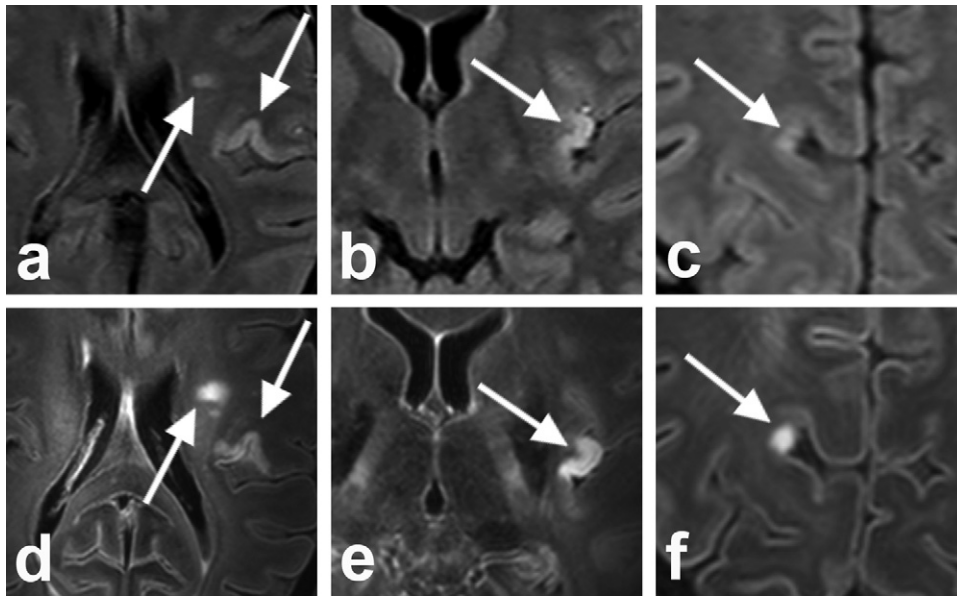


Fig. 5. 40-year-old female with a history of systemic lupus erythematosus (SLE) presented with thrombotic thrombocytopenic purpura (TTP) complicated by transient motor dysphasia. a–c, Axial standard clinical 1.5 T and d–f, corresponding 7 T MRI FLAIR images, showing several small cortical and subcortical hyperintense ischemic lesions (arrows). Due to the higher contrast-to-noise ratio at 7 T, lesions were more conspicuous than at lower field strength, and some were seen only in retrospect at 1.5 T (arrow in c, compared to f). Imaging parameters as previously published [3], 0.8 mm isotropic resolution.

3.5. Epilepsy

7 T MRI may give additional diagnostic information in patients with cryptogenic epilepsy in which no structural epileptic focus can be found at 3 T and 1.5 T. With the improved SNR and possibility of scanning at a high spatial resolution, it may be possible to

detect small areas of cortical dysplasia at 7 T MRI which may have been missed at lower field strengths, although no such studies have been performed thus far. There are however a few studies which focus on other causes of epilepsy, like cerebral cavernous haemangiomas (CCHs) and hippocampal sclerosis. Two studies assessed CCHs with T_2^* -weighted imaging at 7 T MRI [53,54], of which one

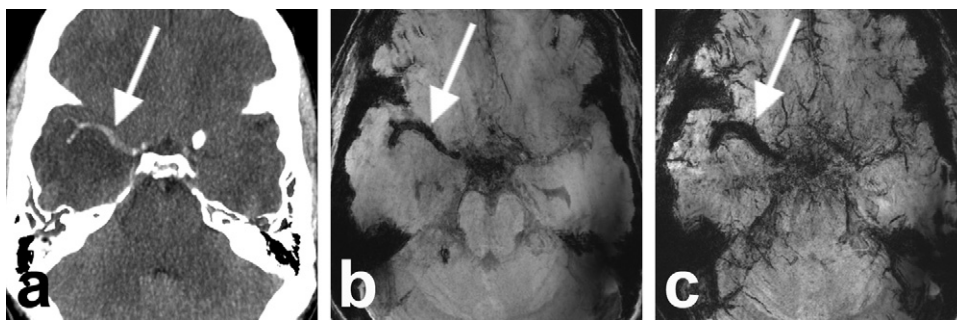


Fig. 6. 42-year-old man with blank medical history presented with searing headache and thereafter hemiparesis of the left arm and leg, based on an ischemic infarction of the right middle cerebral artery (MCA)-territory. a, Axial CT-image showing slightly hypodense signal of the right temporal lobe, as well as a hyperdense vessel sign (arrow) of the right MCA. b, Axial minMIP (over 10 mm thick volume) of the 1st and c, the 2nd echo of 7 T T_2^* -weighted images, visualizing thrombotic material in the right MCA (arrows). Due to the very short T_2^* of thrombus, it can already be seen on the 1st echo minMIP (b). Imaging parameters of the 7 T T_2^* -sequence as previously published [33].

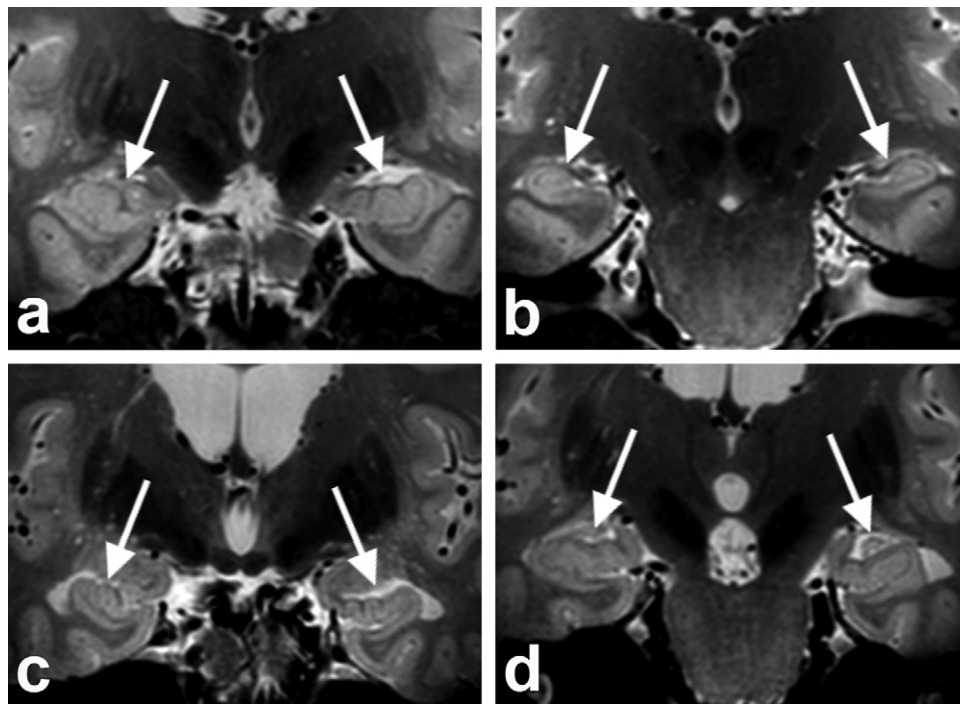


Fig. 7. Coronal images of two healthy volunteers of 41 (a, b) and 77 years old (c, d), showing the head and body of the hippocampus. Although the hippocampal substructures are more readily appreciated in the older volunteer (c, d) due to better contrast between the hippocampal substructures and enlarged cerebrospinal fluid spaces, also in the young volunteer hippocampal substructures can easily be discerned (a, b). Several cortical and subcortical foldings can be identified in both hippocampi and cortical layers. Imaging parameters were TR 3158 ms, TE 271 ms, TSE factor 181, NSA 2, resolution 0.6 mm × 0.7 mm × 0.7 mm.

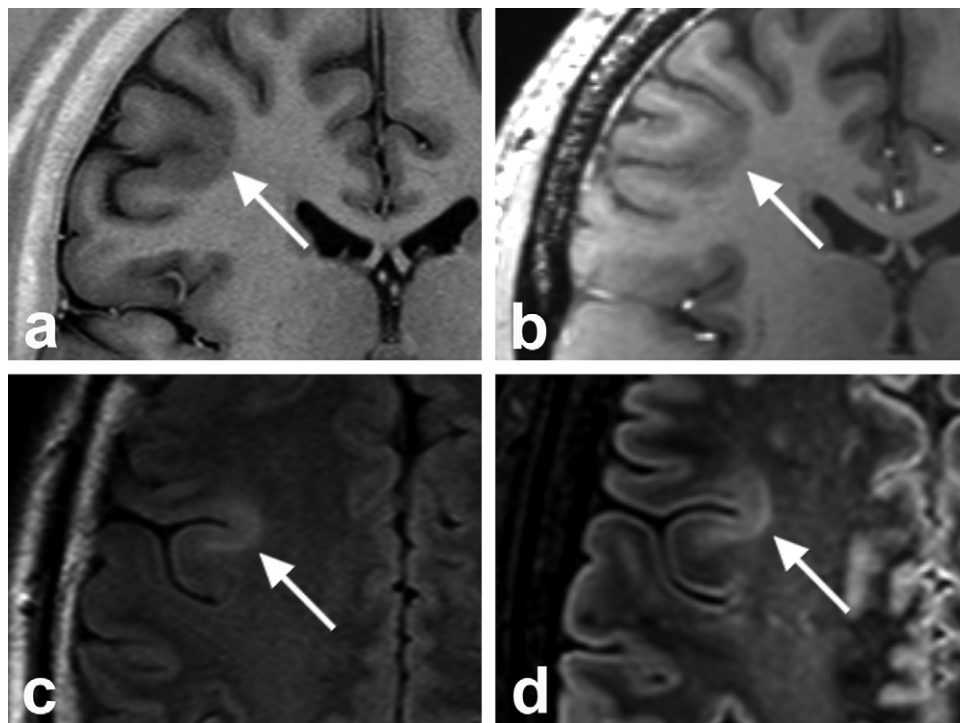


Fig. 8. A 32-year-old male presented with symptomatic therapy-resistant epilepsy characterized by recurrent partial secondary generalized seizures and recurrent status epilepticus. a, Standard clinical 1.5T T_1 -weighted and c, FLAIR image, with corresponding images at 7T MRI (b, d). Both imaging sequences at both field strengths could visualize focal cortical dysplasia medially in the right frontal hemisphere (arrows in a–d). However, due to the higher contrast at 7T, the focal lesion was more pronounced at the 7T FLAIR image (d). Imaging parameters of the 7T FLAIR-sequence as previously published [3]; 7T T_1 -weighted sequence: shot interval 3500 ms, TI 1200 ms, TR 7.0 ms, TE 2.9 ms, 0.8 mm isotropic resolution.

Courtesy of Dr. C.H. Ferrier, UMC Utrecht, The Netherlands.

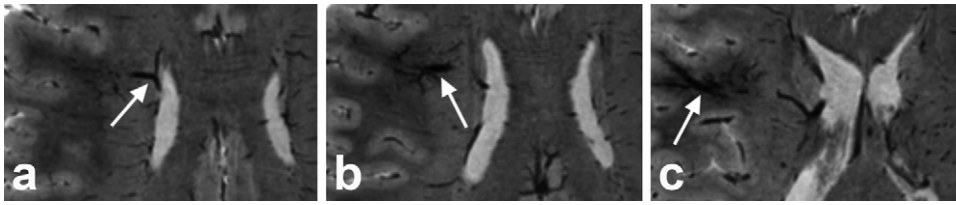


Fig. 9. a–c, Axial 1st echo minMIPs (over 10 mm thick volumes) of T_2^* -weighted 7T MR images of a 22-year-old healthy female volunteer showing a developmental venous anomaly, a benign condition not requiring any treatment if asymptomatic [58]. Due to the increased susceptibility effect of venous deoxygenated blood at high magnetic field, the venous structure can be assessed even at a TE = 2.5 ms, as well as its various branches (arrow in a–c). Imaging parameters as previously published [33].

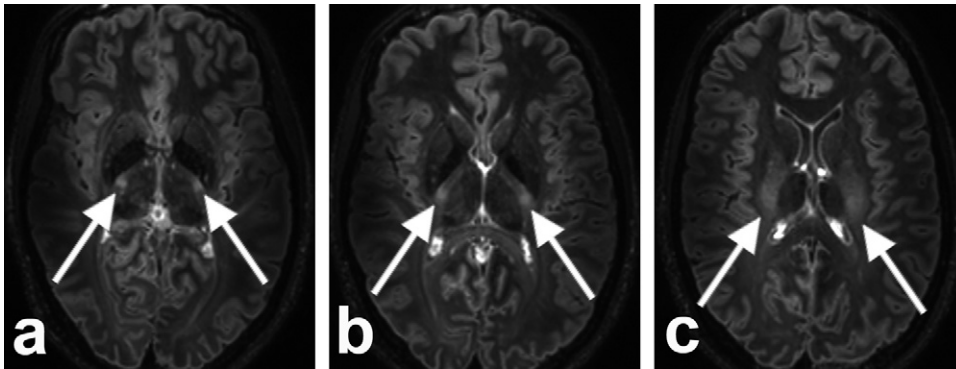


Fig. 10. a–c, Axial reformats of a 3D FLAIR dataset of a 26-year-old healthy female volunteer, showing, among others, the basal ganglia, choroid plexus (hyperintense signals in the ventricles) and the corticospinal tract (arrows) as it ascends to form the internal capsule (b) and then fans out throughout both hemispheres (c). Imaging parameters as previously published [3], 0.8 mm isotropic resolution.

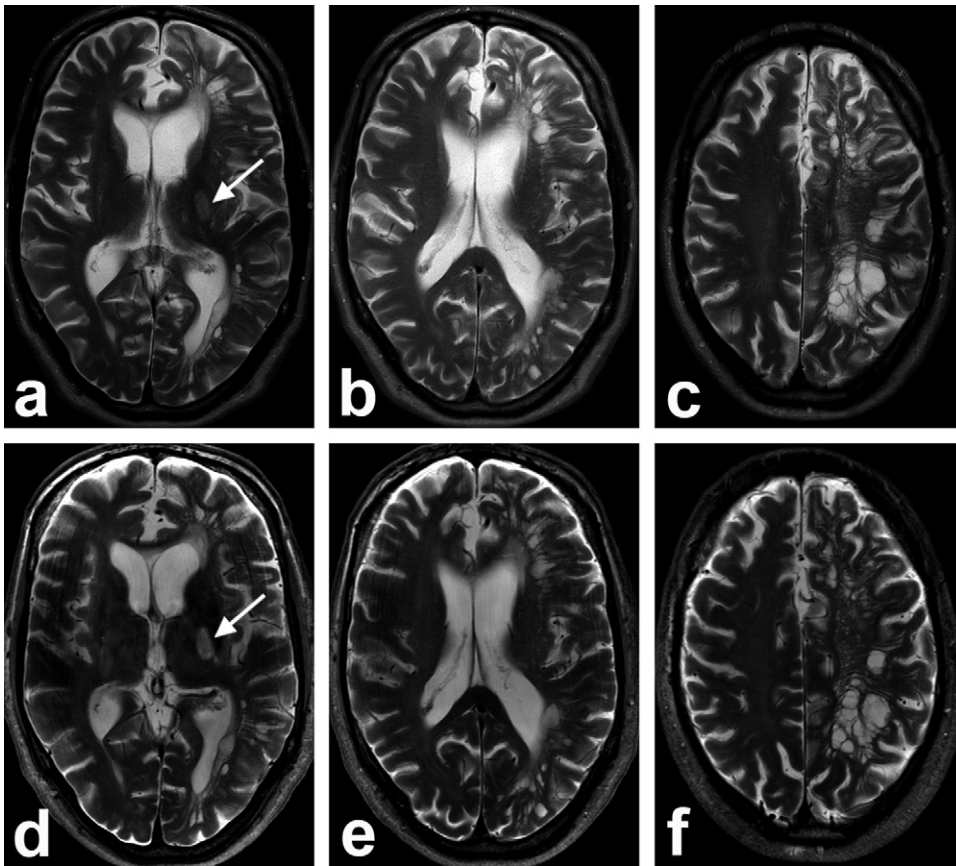


Fig. 11. 61-year-old male with a blank medical history presented with mild dysphasia and hemiparesis of his right arm and leg based on an ischemic stroke of the left hemisphere. a–c, Axial standard clinical 1.5T and d–f, 7T T_2 -weighted MR images, showing the ischemic area at the transition corona radiata – internal capsule (arrows in a and d), which can be more easily appreciated at the 7T images (d). Furthermore, several hyperintense structures can be seen on both 1.5 and 7T localized to the left hemisphere, consistent with enlarged perivascular spaces (a–f). Imaging parameters T_2 -weighted sequence: TR 5828 ms, TE 60 ms, 0.5 mm × 0.7 mm × 4.0 mm resolution.

study compared their results with images obtained at 1.5 T MRI [53]. They found that 7 T MRI resulted in identification of more cavernomas than at 1.5 T, suggesting that 7 T MRI might be of additional diagnostic value [53]. Another study compared 1.5 T with 7 T MRI for imaging hippocampal sclerosis, and found that 7 T provided better delineation of anatomical hippocampal structures by means of strong contrast, potentially improving detection of structural changes causing epileptic seizures [55]. An initial study with postoperative specimens with focal cortical dysplasia showed the correlation between 7 T MRI findings and pathology [56]. Future studies will show the additional diagnostic value of 7 T MRI in detection of epileptic lesions not currently seen at lower field strengths.

3.6. Other diseases and accidental findings

7 T MRI may also be of benefit in more generalized changes of the brain, for instance less specific changes associated with aging. The most obvious changes associated with aging are atrophy and increased white matter lesions and (silent) infarcts. 7 T MRI with high resolution imaging of the cerebral cortex may show more clearly the extent of changes in the brain tissue, even in brain regions that may appear normal at 3 T and 1.5 T MRI. Furthermore, detection of associated changes in or close to the brain vasculature may give clues as to possible causes of brain tissue changes associated with aging. In addition to aging-related findings, the number of chance findings may also increase when performing 7 T MRI with a high spatial resolution. Especially with T_2^* -weighted imaging, detection of developmental venous anomalies (DVAs) may increase due to the more pronounced visualization of the veins at 7 T. These and other clearly benign lesions should not be mistaken for pathology. Finally, for radiologists the different tissue contrasts at 7 T may result in a learning curve to find out a new normal reference. For instance the basal ganglia and the white matter may show more extensive internal structures at 7 T MRI that are not present at lower field strengths [57].

4. Case series

Illustrative case examples of patients within the previously mentioned disease categories can be found in Figs. 2–11. All patients gave written informed consent to be scanned at 7 T MRI at the University Medical Center Utrecht, The Netherlands, in accordance with the guidelines of our institutional review board. All 7 T imaging was performed on a 7.0 T whole body scanner (Philips Healthcare, Cleveland, OH, USA) with a 16 channel receive coil and volume transmit/receive coil for transmission (Nova Medical, Wilmington, MA, USA).

5. Conclusions

The field of clinical 7 T MRI of the brain is moving forward quickly, and several technical developments, like 7 T FLAIR, T_2^* -weighted imaging and high-resolution MRA, have the potential of being applied in the near future in various disease categories. Using the high SNR and CNR obtained with high field imaging, we may gain important insights that at present are not obtained with lower field strengths, regarding the pathophysiology, diagnosis, and treatment of several disease entities, such as MS, brain tumours, and epilepsy. It is, however, important to determine the actual diagnostic and prognostic value of these new findings obtained with 7 T MRI. Especially, the advantages of high field imaging for clinical diagnosis and treatment should be weighted against the potential disadvantages of inhomogeneous transmit fields and patient contraindications. In this regard, studies comparing 7 T MRI

with imaging at lower field strengths will be needed to address this clinically relevant question.

Disclosures

Fredy Visser is employee of Philips Healthcare, Best, The Netherlands.

References

- [1] Cha S, Gore JC. Clinical applications of ultra-high field 7 T MRI – moving to FDA/EU approval. In: Proc. Intl. Soc. Mag. Reson. Med. 19. 2011.
- [2] Ladd ME, van Buchem MA, Rinck PA. Hot topics debate “Can 7 T Go Clinical?”. In: Proc. Intl. Soc. Mag. Reson. Med. 18. 2010.
- [3] Visser F, Zwanenburg JJ, Hoogduin JM, Luijten PR. High-resolution magnetization-prepared 3D-FLAIR imaging at 7.0 Tesla. *Magn Reson Med* 2010;64(1):194–202.
- [4] Thomas BP, Welch EB, Niederhauser BD, et al. High-resolution 7 T MRI of the human hippocampus in vivo. *J Magn Reson Imaging* 2008;28(5):1266–72.
- [5] Zwanenburg JJ, Versluis MJ, Luijten PR, Petridou N. Fast high resolution whole brain T_2^* -weighted imaging using echo planar imaging at 7 T. *Neuroimage* 2011;56(4):1902–7.
- [6] Van de Moortele PF, Auerbach EJ, Olman C, Yacoub E, Ugurbil K, Moeller S. T1 weighted brain images at 7 Tesla unbiased for proton density, T_2^* contrast and RF coil receive B1 sensitivity with simultaneous vessel visualization. *Neuroimage* 2009;46(2):432–46.
- [7] Bottomley PA, Foster TH, Argersinger RE, Pfeifer LM. A review of normal tissue hydrogen NMR relaxation times and relaxation mechanisms from 1–100 MHz: dependence on tissue type, NMR frequency, temperature, species, excision, and age. *Med Phys* 1984;11(4):425–48.
- [8] Rooney WD, Johnson G, Li X, et al. Magnetic field and tissue dependencies of human brain longitudinal $1H_2O$ relaxation in vivo. *Magn Reson Med* 2007;57(2):308–18.
- [9] van der Kolk AG, Zwanenburg JJ, Brundel M, et al. Intracranial vessel wall imaging at 7.0 Tesla MRI. *Stroke* 2011;42(9):2478–84.
- [10] Vaughan JT, Garwood M, Collins CM, et al. 7 T vs. 4 T: RF power, homogeneity, and signal-to-noise comparison in head images. *Magn Reson Med* 2001;46(1):24–30.
- [11] Collins CM, Liu W, Wang J, et al. Temperature and SAR calculations for a human head within volume and surface coils at 64 and 300 MHz. *J Magn Reson Imaging* 2004;19(5):650–6.
- [12] Rudick RA, Trapp BD. Gray-matter injury in multiple sclerosis. *N Engl J Med* 2009;361(15):1505–6.
- [13] Zwanenburg JJ, Hendrikse J, Visser F, Takahara T, Luijten PR. Fluid attenuated inversion recovery (FLAIR) MRI at 7.0 Tesla: comparison with 1.5 and 3.0 Tesla. *Eur Radiol* 2010;20(4):915–22.
- [14] de Graaf WL, Visser F, Wattjes MP, et al. 7 Tesla 3D-FLAIR and 3D-DIR: high sensitivity in cortical regions in multiple sclerosis. In: Proc. Intl. Soc. Mag. Reson. Med. 18. 2010.
- [15] Hammond KE, Metcalf M, Carvajal L, et al. Quantitative in vivo magnetic resonance imaging of multiple sclerosis at 7 Tesla with sensitivity to iron. *Ann Neurol* 2008;64(6):707–13.
- [16] Kollia K, Maderwald S, Putzki N, et al. First clinical study on ultra-high-field MR imaging in patients with multiple sclerosis: comparison of 1.5 T and 7 T. *AJNR Am J Neuroradiol* 2009;30(4):699–702.
- [17] Mainero C, Benner T, Radding A, et al. In vivo imaging of cortical pathology in multiple sclerosis using ultra-high field MRI. *Neurology* 2009;73(12):941–8.
- [18] Tallantyre EC, Morgan PS, Dixon JE, et al. 3 Tesla and 7 Tesla MRI of multiple sclerosis cortical lesions. *J Magn Reson Imaging* 2010;32(October (4)):971–7.
- [19] Tallantyre EC, Brookes MJ, Dixon JE, Morgan PS, Evangelou N, Morris PG. Demonstrating the perivascular distribution of MS lesions in vivo with 7-Tesla MRI. *Neurology* 2008;70(22):2076–8.
- [20] Ge Y, Zohrabian VM, Grossman RI. Seven-Tesla magnetic resonance imaging: new vision of microvascular abnormalities in multiple sclerosis. *Arch Neurol* 2008;65(6):812–6.
- [21] Tallantyre EC, Morgan PS, Dixon JE, et al. A comparison of 3 T and 7 T in the detection of small parenchymal veins within MS lesions. *Invest Radiol* 2009;44(9):491–4.
- [22] Tallantyre EC, Dixon JE, Donaldson I, et al. Ultra-high-field imaging distinguishes MS lesions from asymptomatic white matter lesions. *Neurology* 2011;76(6):534–9.
- [23] Lucchinetti C, Bruck W, Parisi J, Scheithauer B, Rodriguez M, Lassmann H. Heterogeneity of multiple sclerosis lesions: implications for the pathogenesis of demyelination. *Ann Neurol* 2000;47(6):707–17.
- [24] Kang CK, Park CW, Han JY, et al. Imaging and analysis of lenticulostriate arteries using 7.0-Tesla magnetic resonance angiography. *Magn Reson Med* 2009;61(1):136–44.
- [25] Cho ZH, Kang CK, Han JY, et al. Observation of the lenticulostriate arteries in the human brain in vivo using 7.0 T MR angiography. *Stroke* 2008;39(5):1604–6.
- [26] Zwanenburg JJ, Hendrikse J, Takahara T, Visser F, Luijten PR. MR angiography of the cerebral perforating arteries with magnetization prepared anatomical reference at 7 T: comparison with time-of-flight. *J Magn Reson Imaging* 2008;28(6):1519–26.

- [27] Wardlaw JM. Blood–brain barrier and cerebral small vessel disease. *J Neurol Sci* 2010;299(1–2):66–71.
- [28] Kang CK, Park CA, Park CW, Lee YB, Cho ZH, Kim YB. Lenticulostriate arteries in chronic stroke patients visualised by 7T magnetic resonance angiography. *Int J Stroke* 2010;5(5):374–80.
- [29] Kang CK, Park CA, Lee H, et al. Hypertension correlates with lenticulostriate arteries visualized by 7T magnetic resonance angiography. *Hypertension* 2009;54(5):1050–6.
- [30] Liem MK, van der Grond J, Versluis MJ, et al. Lenticulostriate arterial lumina are normal in cerebral autosomal-dominant arteriopathy with subcortical infarcts and leukoencephalopathy. A high-field in vivo MRI study. *Stroke* 2010;41(12):2812–6.
- [31] Monninghoff C, Maderwald S, Wanke I. Pre-interventional assessment of a vertebrobasilar aneurysm with 7 Tesla time-of-flight MR angiography. *Rofo* 2009;181(3):266–8.
- [32] Monninghoff C, Maderwald S, Theysohn JM, et al. Evaluation of intracranial aneurysms with 7T versus 1.5 T time-of-flight MR angiography – initial experience. *Rofo* 2009;181(1):16–23.
- [33] Conijn MM, Geerlings MI, Luijten PR, et al. Visualization of cerebral microbleeds with dual-echo T_2^* -weighted magnetic resonance imaging at 7.0T. *J Magn Reson Imaging* 2010;32(1):52–9.
- [34] Conijn MM, Geerlings MI, Biessels GJ, et al. Cerebral microbleeds on MR imaging: comparison between 1.5 and 7T. *AJNR Am J Neuroradiol* 2011;32(6):1043–9.
- [35] Biessels GJ, Zwanenburg JJ, Visser F, Frijns CJ, Luijten PR. Hypertensive cerebral hemorrhage: imaging the leak with 7-T MRI. *Neurology* 2010;75(6):572–3.
- [36] Swartz RH, Bhuta SS, Farb RI, et al. Intracranial arterial wall imaging using high-resolution 3-Tesla contrast-enhanced MRI. *Neurology* 2009;72(7):627–34.
- [37] Ryu CW, Jahng GH, Kim EJ, Choi WS, Yang DM. High resolution wall and lumen MRI of the middle cerebral arteries at 3Tesla. *Cerebrovasc Dis* 2009;27(5):433–42.
- [38] Xu WH, Li ML, Gao S, et al. In vivo high-resolution MR imaging of symptomatic and asymptomatic middle cerebral artery atherosclerotic stenosis. *Atherosclerosis* 2010;212(2):507–11.
- [39] Theysohn JM, Kraff O, Maderwald S, et al. 7Tesla MRI of microbleeds and white matter lesions as seen in vascular dementia. *J Magn Reson Imaging* 2011;33(4):782–91.
- [40] Dierksen GA, Skehan ME, Khan MA, et al. Spatial relation between microbleeds and amyloid deposits in amyloid angiopathy. *Ann Neurol* 2010;68(4):545–8.
- [41] van Rooden S, Maat-Schieman ML, Nabuurs RJ, et al. Cerebral amyloidosis: postmortem detection with human 7.0-T MR imaging system. *Radiology* 2009;253(3):788–96.
- [42] Versluis MJ, Peeters JM, van Rooden S, et al. Origin and reduction of motion and f0 artifacts in high resolution T_2^* -weighted magnetic resonance imaging: application in Alzheimer's disease patients. *Neuroimage* 2010;51(3):1082–8.
- [43] Theysohn JM, Kraff O, Maderwald S, et al. The human hippocampus at 7T – in vivo MRI. *Hippocampus* 2009;19(1):1–7.
- [44] Kerchner GA, Hess CP, Hammond-Rosenbluth KE, et al. Hippocampal CA1 apical neuropil atrophy in mild Alzheimer disease visualized with 7-T MRI. *Neurology* 2010;75(15):1381–7.
- [45] Cho ZH, Min HK, Oh SH, et al. Direct visualization of deep brain stimulation targets in Parkinson disease with the use of 7-Tesla magnetic resonance imaging. *J Neurosurg* 2010;113(3):639–47.
- [46] Bajaj N, Schafer A, Wharton S, et al. PATH53 Magnetic susceptibility of substantia nigra in Parkinson's disease: a 7-T in vivo MRI study. *J Neurol Neurosurg Psychiatry* 2010;81(11):e22.
- [47] Oh SH, Kim JM, Park SY, et al. Direct visualization of Parkinson's disease by in vivo human brain imaging using 7.0T MRI. In: *Proc. Intl. Soc. Mag. Reson. Med.* 19. 2011. p. 2181.
- [48] Moenninghoff C, Maderwald S, Theysohn JM, et al. Imaging of adult astrocytic brain tumours with 7T MRI: preliminary results. *Eur Radiol* 2010;20(3):704–13.
- [49] Moenninghoff C, Maderwald S, Theysohn JM, et al. Imaging of brain metastases of bronchial carcinomas with 7T MRI – initial results. *Fortschr Röntgenstr* 2010;182:764–72.
- [50] Moenninghoff C, Kraff O, Schlamann M, Ladd ME, Katsarava Z, Gizewski ER. Assessing a dysplastic cerebellar gangliocytoma (Lhermitte-Duclos disease) with 7T MR imaging. *Korean J Radiol* 2010;11(2):244–8.
- [51] Nath K, Agarwal M, Ramola M, et al. Role of diffusion tensor imaging metrics and in vivo proton magnetic resonance spectroscopy in the differential diagnosis of cystic intracranial mass lesions. *Magn Reson Imaging* 2009;27(2):198–206.
- [52] Lupo JM, Banerjee S, Hammond KE, et al. GRAPPA-based susceptibility-weighted imaging of normal volunteers and patients with brain tumor at 7T. *Magn Reson Imaging* 2009;27(4):480–8.
- [53] Schlamann M, Maderwald S, Becker W, et al. Cerebral cavernous hemangiomas at 7 Tesla: initial experience. *Acad Radiol* 2010;17(1):3–6.
- [54] Dammann P, Barth M, Zhu Y, et al. Susceptibility weighted magnetic resonance imaging of cerebral cavernous malformations: prospects, drawbacks, and first experience at ultra-high field strength (7-Tesla) magnetic resonance imaging. *Neurosurg Focus* 2010;29(3):E5.
- [55] Breyer T, Wanke I, Maderwald S, et al. Imaging of patients with hippocampal sclerosis at 7 Tesla: initial results. *Acad Radiol* 2010;17(4):421–6.
- [56] Garbelli R, Zucca I, Milesi G, et al. Combined 7-T MRI and histopathologic study of normal and dysplastic samples from patients with TLE. *Neurology* 2011;76(13):1177–85.
- [57] Li TQ, Yao B, van Gelderen P, et al. Characterization of $T(2)^*$ heterogeneity in human brain white matter. *Magn Reson Med* 2009;62(6):1652–7.
- [58] Lasjaunias P, Burrows P, Planet C. Developmental venous anomalies (DVA): the so-called venous angioma. *Neurosurg Rev* 1986;9(3):233–42.